

# Viscoelastic Fluid Flows at Moderate Weissenberg Numbers Using Oldroyd Type Model

L. Pirkel\*, T. Bodnár\*,† and K. Tůma\*\*

\*Department of Technical Mathematics, Faculty of Mechanical Engineering, Czech Technical University, Karlovo náměstí 13, 121 35 Prague 2, Czech Republic

†Institute of Thermomechanics, Academy of Sciences of Czech Republic, Dolejšková 5, 182 00 Prague 8, Czech Republic

\*\*Mathematical Institute, Charles University, Sokolovská 83, 186 75 Prague 8, Czech Republic

**Abstract.** This paper presents the preliminary results of our numerical simulations designed and performed to address the high Weissenberg number problem that is the major challenge in the simulation of viscoelastic flows. The mathematical model used to explore this problem is based on Oldroyd type model. A new simple computational test case is proposed and solved to demonstrate the nature of the high Weissenberg number problem. Various finite-volume as well as finite-element methods are introduced to be tested for this test case. Some of our very first results are presented and discussed at the end.

**Keywords:** non-Newtonian, viscoelastic, Oldroyd-B, finite-volume

**PACS:** 47.11.Df, 47.50.Cd, 47.63.Cb, 87.19.U-, 87.85.gf

## INTRODUCTION

The simulations of viscoelastic fluid flows using Oldroyd-B model present a challenging problem. The major difficulties appear at high Weissenberg numbers, where most of the simulations fail to converge. This issue has been (and still is) addressed by many scientists working in non-Newtonian CFD. Some of the recent contributions in this area can be found e.g. in [1] and [2]. The nature of the high Weissenberg number problem is not easy to formulate. It should be seen from at least three different points of view. Physically, the increase of Weissenberg number corresponds to growth of *relaxation time* and thus the ability of the fluid to “remember” and accumulate stress. Thus the flow is more affected by the stress history. From the mathematical point of view, it seems that the underlying governing PDEs are changing their type and therefore it is more difficult to analyse the solution behaviour and guarantee its convergence at certain regimes. And last, but not least, from the numerical point of view the problem becomes also hard to solve especially due to presence of large solution gradients and presence of some specific solution instabilities.

## MATHEMATICAL MODEL

The model is based on basic conservation laws of mass and momentum for incompressible fluid flows. These are represented by the continuity equation (divergence free constraint) (1) and the momentum equations (2).

$$\operatorname{div} \mathbf{u} = 0 \quad (1)$$

$$\rho \dot{\mathbf{u}} = \operatorname{div} \mathbf{T} - \nabla p \quad (2)$$

Here  $\mathbf{u}$  stands for the velocity vector,  $\rho$  is density,  $p$  is pressure. The stress tensor is denoted by  $\mathbf{T}$ . In the case of a Newtonian fluid the stress tensor  $\mathbf{T}$  is proportional to symmetric part of the velocity gradient  $\mathbf{D} = (\nabla \mathbf{u} + \nabla \mathbf{u}^T)/2$ , i.e.  $\mathbf{T} = 2\mu \mathbf{D}$ . The dynamic viscosity  $\mu$  is usually assumed to be constant. For the study presented here the rheological model is based on the Oldroyd-type model often referred to as the *Johnson-Segalman* model. The well known upper-, lower- and co-rotational Maxwell models as well as the Oldroyd-A and Oldroyd-B models are just special sub-cases of the Johnson-Segalman class of models.

Stress tensor  $\mathbf{T} = \mathbf{T}_s + \mathbf{T}_e$  consists of the Newtonian (solvent) part  $\mathbf{T}_s$  and the viscoelastic part  $\mathbf{T}_e$ . These two stress components  $\mathbf{T}_s$  and  $\mathbf{T}_e$  are defined as follows.

$$\mathbf{T}_s = 2\mu_s \mathbf{D} \quad (3)$$

$$\mathbf{T}_e + \lambda \frac{\delta \mathbf{T}_e}{\delta t} = 2\mu_e \mathbf{D} \quad (4)$$

The symbol  $D$  denotes the symmetric part of the velocity gradient. The physical parameters in this model are the solvent and elastic viscosities  $\mu_s$ , resp.  $\mu_e$  and the relaxation time  $\lambda$ .

The *convected derivative*  $\frac{\delta \mathbf{T}_e}{\delta t}$  in the equation (4) can be chosen from the one-parametric family of *Gordon-Schowalter* derivatives given by :

$$\left( \frac{\delta \mathbf{T}_e}{\delta t} \right)_a = \dot{\mathbf{T}}_e - \mathbf{W} \mathbf{T}_e + \mathbf{T}_e \mathbf{W} + a(\mathbf{D} \mathbf{T}_e + \mathbf{T}_e \mathbf{D}) \quad a \in \langle -1; 1 \rangle \quad (5)$$

For  $a = -1$ , this leads to upper convected derivative,  $a = 0$  gives co-rotational (or Jaumann) derivative and for  $a = 1$  we get the lower convected derivative. The most commonly used Oldroyd-B (upper convected Maxwell) model is obtained for  $a = -1$ .

$$\frac{\partial \mathbf{T}_e}{\partial t} + (\mathbf{u} \cdot \nabla) \mathbf{T}_e = \frac{2\mu_e}{\lambda} \mathbf{D} - \frac{1}{\lambda} \mathbf{T}_e + (\mathbf{W} \mathbf{T}_e - \mathbf{T}_e \mathbf{W}) - a(\mathbf{D} \mathbf{T}_e + \mathbf{T}_e \mathbf{D}) \quad a \in \langle -1; 1 \rangle \quad (6)$$

Besides of the geometrical parameters, the flow is defined by the following physical parameters to be prescribed:

$$U, \rho, \mu_s, \mu_e, \lambda$$

Using the characteristic velocity  $U$ , tube diameter  $D$  and total viscosity  $\mu = \mu_s + \mu_e$ , the *Reynolds number* and *Weissenberg number* can be determined as

$$Re = \frac{\rho U D}{\mu} \quad \text{and} \quad We = \frac{\lambda U}{D}$$

The last dimensionless parameter is the *elastic viscosity ratio*  $\alpha = \mu_e / (\mu_s + \mu_e)$ . For the study of high Weissenberg number problem the Reynolds number as well as the viscosity ratio will be kept fixed. The physical parameters are prescribed in the following way:  $D = 0.01 \text{ m}$ ,  $U = 0.1 \text{ m} \cdot \text{s}^{-1}$ ,  $\rho = 1000 \text{ kg} \cdot \text{m}^{-3}$ ,  $\mu_s = 0.009 \text{ kg} \cdot \text{m}^{-1} \cdot \text{s}^{-1}$ ,  $\mu_e = 0.001 \text{ kg} \cdot \text{m}^{-1} \cdot \text{s}^{-1}$ .

This setup leads to fixed Reynolds number  $Re = 100$  and elastic viscosity ratio  $\alpha = 0.9$ . The Weissenberg number will vary proportionally to the relaxation time  $\lambda$  as  $We = 10\lambda$ .

## NUMERICAL METHODS

The problem was solved numerically by two independent groups. The solution approaches have been chosen different by each group.

*Finite-Volume Methods.* Three different finite-volume methodologies have been used. The two in-house built solvers are based on central in space finite-volume discretisations. The 2D solver used Mac-Cormack predictor-corrector method. For the 3D code the system of governing PDEs is first discretised in space by central finite-volume method and consequently the arising system of ODEs is integrated in time using Runge-Kutta multistage scheme. The details can be found in [3, 4]. For comparison, an open source code OpenFOAM was used.

*Finite-Element Methods.* All models are computed using finite element method based on the weak formulation of the governing equations. The computational domain is discretised by regular quadrilaterals. Pressure  $p$ /velocity  $\vec{v}$ /part of the stress  $\mathbf{A}$  are approximated by P1<sup>disc</sup>/Q2/Q2 elements for the Galerkin method. A fully coupled monolithic finite element approach that treats all the numerical variables simultaneously. Both steady and unsteady cases can be solved. The Euler method is used for the unsteady case. No stabilisation is used for the Galerkin method. The stabilising Galerkin/Least-Squares method based on the minimisation of  $L^2$  norm of equation (see [5]) is actually tested as well. The Oldroyd-B model can be also written in the form of conformation tensor which is positive definite. The positive definiteness preserving transformation (see [6]) is used for both Galerkin and GLS method.

## COMPUTATIONAL DOMAIN

The computational geometry consists of a three-dimensional tube with circular crosssection. The crosssectional area diameter varies depending on the axial coordinate. The straight inlet and outlet parts have a constant diameter  $D$ . In between these straight parts, several ( $N_{seg}$ ) identical segments with variable diameter are placed. These segments have cosine-shaped walls with diameter changing from  $D_{min}$  to  $D_{max}$ . The length  $L_{seg}$  of the segment and the number of

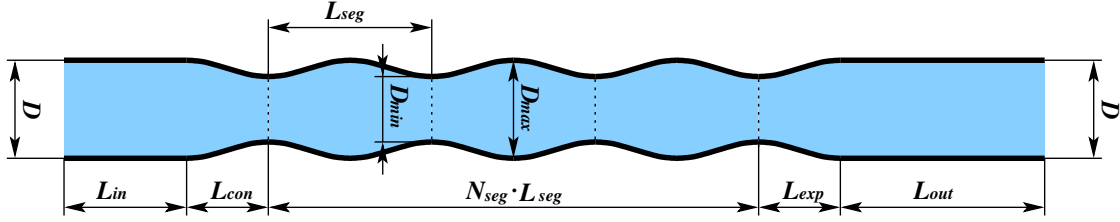


FIGURE 1. Problem geometry configuration

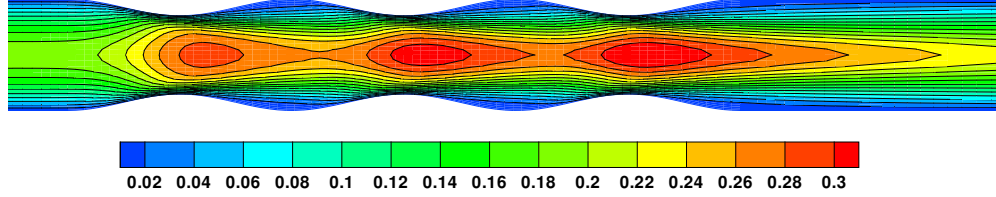


FIGURE 2. Axial velocity contours for the Newtonian fluid flow (i.e. at  $We = 0$ ).

segments  $N_{seg}$  changes from case to case. The variable diameter segments are smoothly attached to the inlet/outlet tubes by cosine shaped contraction/expansion parts. The sketch of a typical computational geometry is shown in the Figure 1. This general computational geometry setup represents a class of problems where the axial and radial length scales can independently be defined. Moreover the periodicity of the geometry allows for easy change of the frequency (by varying  $L_{seg}$ ) and range of loading/unloading of the fluid (by changing the rate  $D_{max}/D_{min}$ ). Thus this test case is extremely well suited for the tests of viscoelastic models and numerical methods for their solution.

*Specific test case configuration.* The general geometrical setup defined above contains 9 independent geometrical parameters. These parameters are  $D$ ,  $D_{max}$ ,  $D_{min}$ ,  $L_{in}$ ,  $L_{out}$ ,  $L_{seg}$ ,  $L_{con}$ ,  $L_{exp}$ ,  $N_{seg}$ . We will further focus our work on tubes with nominal diameter  $D = 1\text{ cm}$  and we will only keep two independent parameters  $L_{seg}$  and  $N_{seg}$  to control the geometry. The other parameters will be linked to our free parameters by the following constraints:

$$D_{max} = D, L_{con} = L_{seg}/2, L_{in} = 3D, D_{min} = D/\sqrt{2}, L_{exp} = L_{seg}/2, L_{out} = 5D$$

## NUMERICAL RESULTS

Only few of the whole set of the numerical results that we have obtained are presented in this short abstract. The numerical method used here is the central finite-volume scheme with explicit Runge-Kutta time-integration that has previously been used in [7], [8]. The test case presented here was chosen to be as simple as possible but allowing to demonstrate the differences between low and moderate Weissenberg number results. The computational geometry has two expanding segments of the length  $2D$  (i.e.  $N_{seg} = 2$ ,  $L_{seg} = 2D$ ). The contours of velocity components for the reference Newtonian flow (with  $We = 0$ ) are shown in the Figure 2 and 3. The moderate Weissenberg number case with  $We = 3$  is shown in the Figure 4 and 5. Obviously the differences between the two solutions are still rather

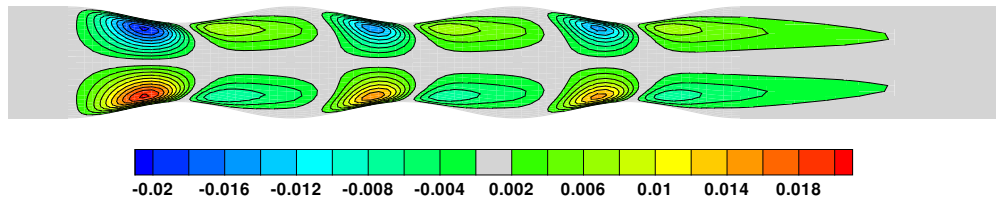


FIGURE 3. Radial velocity contours for the Newtonian fluid flow (i.e. at  $We = 0$ ).

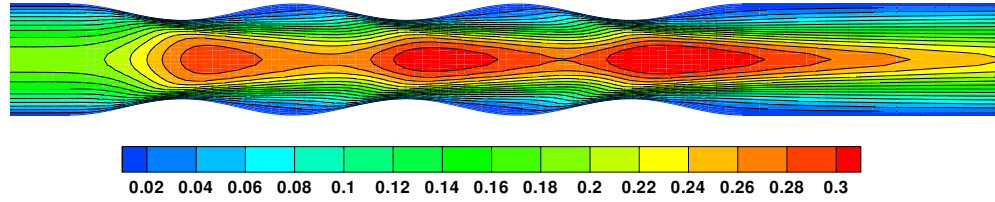


FIGURE 4. Axial velocity contours for the Oldroyd-B fluid flow at  $We = 3$ .

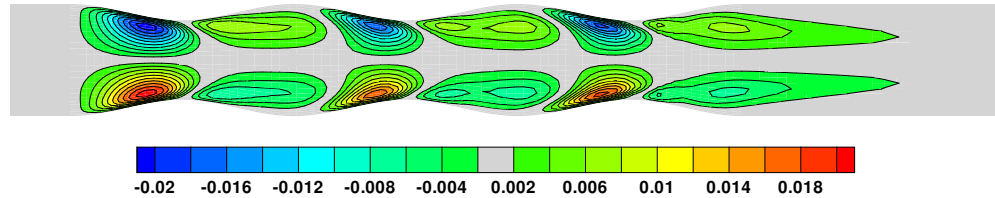


FIGURE 5. Radial velocity contours for the Oldroyd-B fluid flow at  $We = 3$ .

subtle, but already at this stage the ability of the fluid to store and transport the stress starts to play an important role. The viscoelastic fluid needs some time to “relax” the stress. In the case it is repeatedly loaded without having enough time to relax, the stress accumulates. This is manifested in the presented results by the increase of the axial velocity in the last contraction for viscoelastic fluid. Further increase of the Weissenberg number (relaxation time  $\lambda$ ) leads to considerable problems in the numerical solution of this case.

### CONCLUSIONS AND FINAL REMARKS

In this presentation we have established a new test case suitable for testing of viscoelastic fluid flow solvers at moderate and high Weissenberg numbers. The geometry is smooth and axisymmetric. The axial periodicity in the domain shape allows to simulate the situations when the fluid particles are repeatedly loaded and unloaded with predefined frequency and load/unload ratio. The whole test case is steady, but it allows to study the stress accumulation and relaxation along the fluid particle path, that is typical feature of viscoelastic flows that is especially pronounced at high Weissenberg numbers. The numerical results presented here were selected only as a demonstration of expected results for one of the possible test configurations and one of the numerical methods. The results have clearly shown the change of the structure of the solution for growing Weissenberg number. Further work will focus on the comparative study of the presented numerical methods in order to establish a method that will be sufficiently robust and efficient over a large range of Weissenberg numbers.

### ACKNOWLEDGMENTS

The financial support for this work was provided by the *Czech Science Foundation* under the *Grant No.201/09/0917* and *No.201/11/1304* and by the *Research Plan MSM 6840770010* of the Ministry of Education of Czech Republic.

### REFERENCES

1. D. Trebotich, P. Colella, and G. Miller, *Journal of Computational Physics* **205**, 315–342 (2005).
2. M. Hulsen, R. Fattal, and R. Kupferman, *Journal of Non-Newtonian Fluid Mechanics* **127**, 27–39 (2005).
3. T. Bodnár, and A. Sequeira, *Computational and Mathematical Methods in Medicine* **9**, 83–104 (2008).
4. T. Bodnár, A. Sequeira, and L. Pirkel, “Numerical Simulations of Blood Flow in a Stenosed Vessel under Different Flow Rates using a Generalized Oldroyd-B Model,” in *Numerical Analysis and Applied Mathematics*, American Institute of Physics, Melville, New York, 2009, vol. 2.
5. M. Behr, D. Arora, O. Coronado-Matutti, and M. Pasquali, “Stabilized finite element methods of GLS type for Maxwell-B and Oldroyd-B viscoelastic fluids,” in *Proceedings of ECCOMAS 2004*, 2004.
6. H. Damanik, J. Hron, A. Quazzi, and S. Turek, *Journal of Non-Newtonian Fluid Mechanics* **165**, 1105–1113 (2010).
7. T. Bodnár, A. Sequeira, and M. Prosi, *Applied Mathematics and Computation* **217**, 5055–5067 (2011).
8. T. Bodnár, and A. Sequeira, “Numerical Study of the Significance of the Non-Newtonian Nature of Blood in Steady Flow Through a Stenosed Vessel,” in *Advances in Mathematical Fluid Mechanics*, edited by R. Rannacher, and A. Sequeira, Springer Verlag, 2010, pp. 83–104.